nature geoscience

LETTERS

PUBLISHED ONLINE: 20 NOVEMBER 2011 | DOI: 10.1038/NGEO1321

Modern-style plate subduction preserved in the Palaeoproterozoic West African craton

J. Ganne[1]*, V. De Andrade[2,3], R. F. Weinberg[4], O. Vidal[5], B. Dubacq[6], N. Kagambega[7], S. Naba[7], L. Baratoux[1], M. Jessell[1] and J. Allibon[8]

The timing of onset of modern-style plate tectonics is debated. The apparent lack of blueschist metamorphism[1]—a key indicator of modern plate subduction[2]—in rocks aged more than about 1 billion years calls into question the existence of plate tectonics during the Archaean and Palaeoproterozoic eras[3,4]. Instead, plate tectonics and subduction could have either not occurred at that time[5], or could have proceeded differently[6] owing to warmer conditions in the early Earth mantle[7]. Here we use thermodynamic models[8–10] to investigate the formation conditions of metamorphic minerals in the 2.2–2.0 Gyr old West African metamorphic province. We find a record of blueschist metamorphism in these rocks. We show that minerals such as chlorite and phengite formed at high pressures of 10–12 kbar, low temperatures of 400–450 °C and under a geothermal gradient of 10–12 °C km^{-1}. These conditions are typical of modern subduction zones. We therefore suggest that modern-style plate tectonics existed during the Palaeoproterozoic era. We conclude that ancient blueschist metamorphism may exist in other parts of the world, but the identification of these rocks has so far been hampered by methodological problems associated with deciphering their pressure and temperature evolution.

Metamorphic units in Archaean and Palaeoproterozoic cratons, mainly consisting of volcano-sedimentary and volcano-plutonic basins, are most commonly metamorphosed in greenschist facies (generally termed greenstone belts in Archaean terranes), rising to amphibolite facies in the vicinity of granitoids[11]. Precise and accurate pressure–temperature (P–T) estimates of greenschist facies rocks were until very recently out of reach because of the lack of detailed thermodynamic data on phengite and chlorite, two dominant minerals in such rocks. Owing to recent advances in our knowledge of the thermodynamic properties of all endmembers and solid-solution models for chlorite and phengite[12–14], detailed investigations of the thermal evolution of Archaean and Proterozoic greenstone belts are now possible. This approach was tested for a greenstone belt (Fig. 1) cropping out in the Palaeoproterozoic West African craton (WAC).

The southern part of the WAC is dominated by Birimian terrains of Palaeoproterozoic age (about ~2.2–2.0 Gyr old[15]) that extend to the east and the north of the Archaean cratonic nucleus centred on Liberia (Fig. 1). They include narrow volcano-sedimentary basins intruded by linear to arcuate belts of granitoids, from banded tonalite-trondhjemite-granodiorites (TTGs) to leucogranites[16].

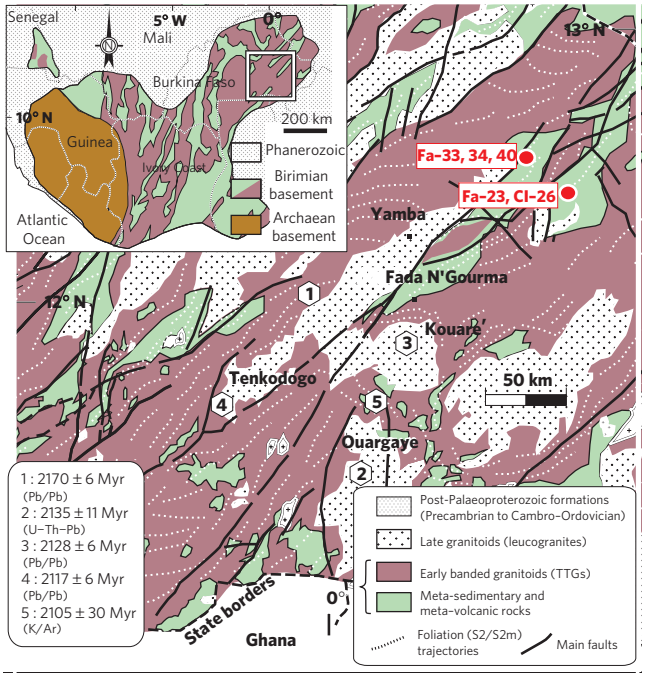

Figure 1 | Geological map of the Fada N'Gourma region. (Modified from ref. 20.) Red circles: location of samples Fa-33 and Fa-34 used for metamorphic modelling. Inset: Location of the Fada N'Gourma greenstone belt in the WAC. The numbered hexagons show geochronological information from previous work (see ref. 20 for more information).

Recent studies[15] concluded that the Birimian units have been initially produced in an immature volcanic arc setting[17] and were later deformed and metamorphosed during the Eburnean orogeny[18,19]. Knowledge of the tectono-thermal evolution of this belt during the Eburnean orogeny (Supplementary Fig. S1) is severely limited by the greenstone belt's poor exposure, which limits our ability to place our samples in a broader structural context, but makes it all the more crucial that we make the most out of the limited number of fresh outcrops and samples.

The belt is interpreted to have undergone a major deformation (D2 event) associated with granitoid intrusions and is responsible for most of the structures observed in the Birimian province[15]. The

[1]IRD, UR 234, GET, Université Toulouse III, 14 Avenue Edouard Belin, 31400 Toulouse, France, [2]NSLS II, Brookhaven National Laboratory, SRX beamline, Bldg 817 Renaissance Road, Upton, New York 11973, USA, [3]European Synchrotron Radiation Facility, ID21 beamline, BP220, 38043 Grenoble Cedex, France, [4]School of Geosciences, Monash University, PO Box 28E, Melbourne, Victoria 3800, Australia, [5]IsTerre, Université J. Fourier, Maison des Géosciences, 1381, rue de la Piscine, 38400 St-Martin d'Hères, France, [6]University of Cambridge, Department of Earth Sciences, Downing Street, Cambridge CB2 3EQ, UK, [7]Département des Géosciences, Université de Ouagadougou, 01 BP 1973 Ouagadougou 01, Burkina Faso, [8]University of Lausanne, Department of Mineralogy and Geochemistry, CH 1015, Lausanne, Switzerland. *e-mail: jerome.ganne@ird.fr.

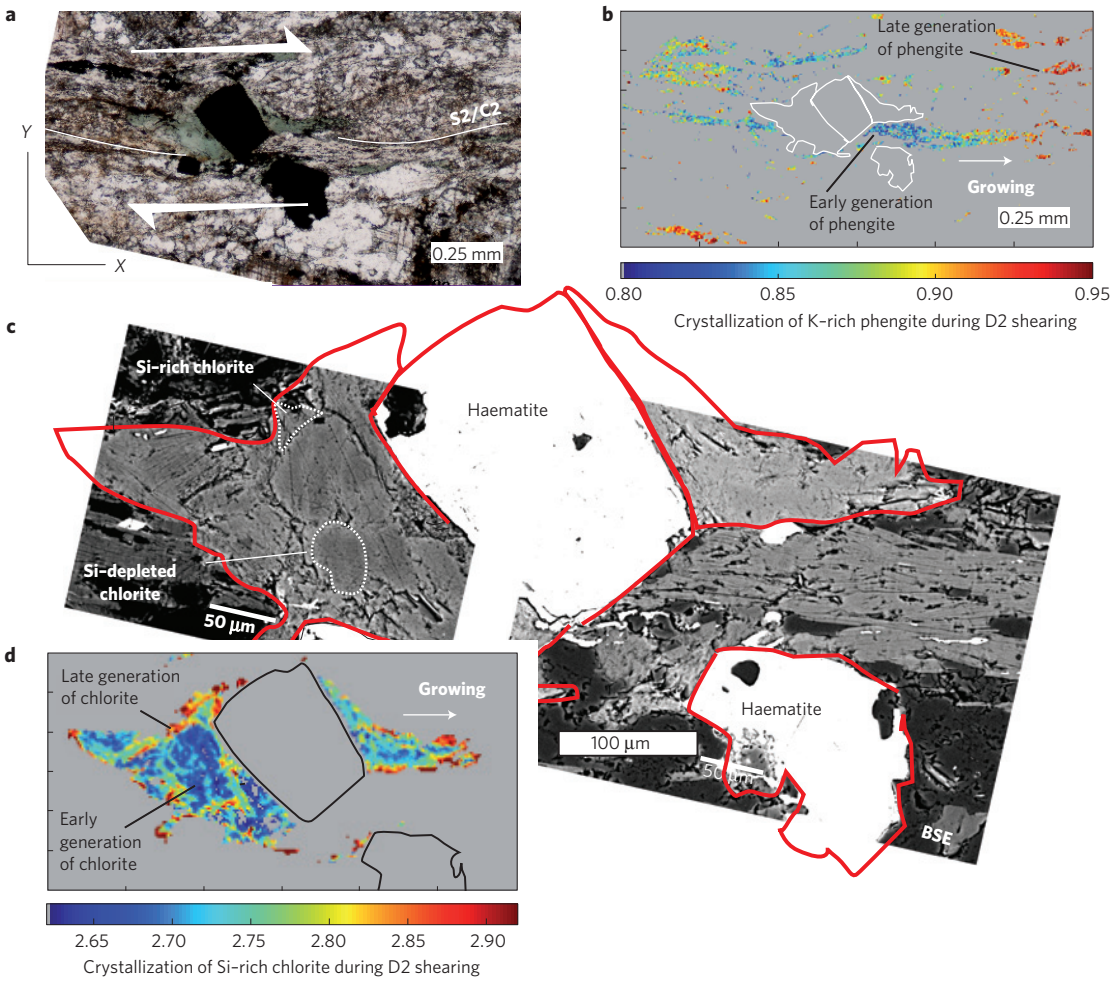

Figure 2 | Chemical evolution of chlorite and phengite during deformation in sample Fa-33. a, Photomicrograph of sample Fa-33. The interpreted dextral sense of shear (white arrows) is based on the asymmetric crystallization tails defined by chlorite. **b**, Distribution of potassium (K)-rich phengite around the crystallization tails, based on compositional mapping. Note the concentration of K-poor phengite (pyrophyllite endmember) growing early at the centre of the tail. **c**, Back-scattered electron (BSE) imaging across the chlorite crystallization tails. **d**, Distribution of silica (Si)-rich chlorite around haematite grains, obtained through compositional mapping. Note the early generation of Si-poor chlorite (amesite endmember) preserved in the core of the tail. Coloured scales correspond to the number of K cations in phengites (**b**) and Si cations in chlorites (**d**).

existence of a remnant S1 fabric, developed early in the Eburnean orogeny, is supported by a few authors[19]. S1 is often described as a crenulated foliation, broadly parallel to (S0) bedding and outlined by low-grade assemblages (chlorite, phengite and carbonates). D2 deformation in the greenstones is characterized by north-northeast- to northeast-trending, steeply dipping (S2) foliation, large-scale (F2) upright synforms and north- to northeast-trending (S2/C2) transcurrent shear zones[15,19]. D2 features in the greenstones have broadly the same orientation as the subvertical foliation (S2m) and compositional layering within granitoids[20] (Fig. 1). They are interpreted to have developed contemporaneously during east–west to west-northwest–east-southeast regional shortening[15,19].

The overall tectonic regime and thermal evolution of the Eburnean orogeny can best be understood by focusing on the temperature-sensitive meta-sedimentary rocks (meta-pelites and meta-greywackes) collected in the thermal aureoles of granitoids (Supplementary Fig. S2). Samples have a strong (S2) foliation parallel to contact assumed to be related to D2. Ten granitoid–greenstone contacts were selected across the Birimian province (Supplementary Table S1), accounting for the range of metamorphism recorded from low- to high-T conditions. Meta-sedimentary rocks (Fa-23, Fa-33, Fa-34 and Fa-40) and meta-volcanites (CI-26) were collected in the low-T thermal aureoles of granitoids (Fada N'Gourma, Burkina Faso, Fig. 1). The greenschist paragenesis (chlorite–phengite–albite–epidote–calcite–ankerite–ilmenite–haematite–quartz) is widely observed in the rocks (Fig. 2a). Perple-X pseudosections (ref. 21) did not permit us to precisely constrain the shape of the P–T path related to the greenschist event that involved high-variance parageneses. To avoid this technical limitation, the complementary approach of multi-equilibrium calculation[22,23] was used (Supplementary Figs S3–S6) constrained by microstructural observations carried out at the thin-section scale (Fig. 2c). Chemical composition maps at this scale yielded evidence that rocks recorded a composite greenschist facies evolution with development of distinct generations of phengite (Fig. 2b) and chlorite (Fig. 2d).

Following a new procedure detailed in the Methods, five nearly continuous P–T paths were computed for the samples of the Fada N'Gourma area (Supplementary Figs S7 and S8). Three groups of chlorite/phengite assemblage (GpA, GpB and GpC), equilibrated in different ranges of pressure and temperature conditions, have been identified along the P–T path calculated for sample Fa-33 (Fig. 3a). The distribution and proportion of each P–T group was investigated at the thin-section scale, by deriving P–T deformation maps from the chemical composition images of Fa-33 (Fig. 3b,c). The highest metamorphic conditions are recorded

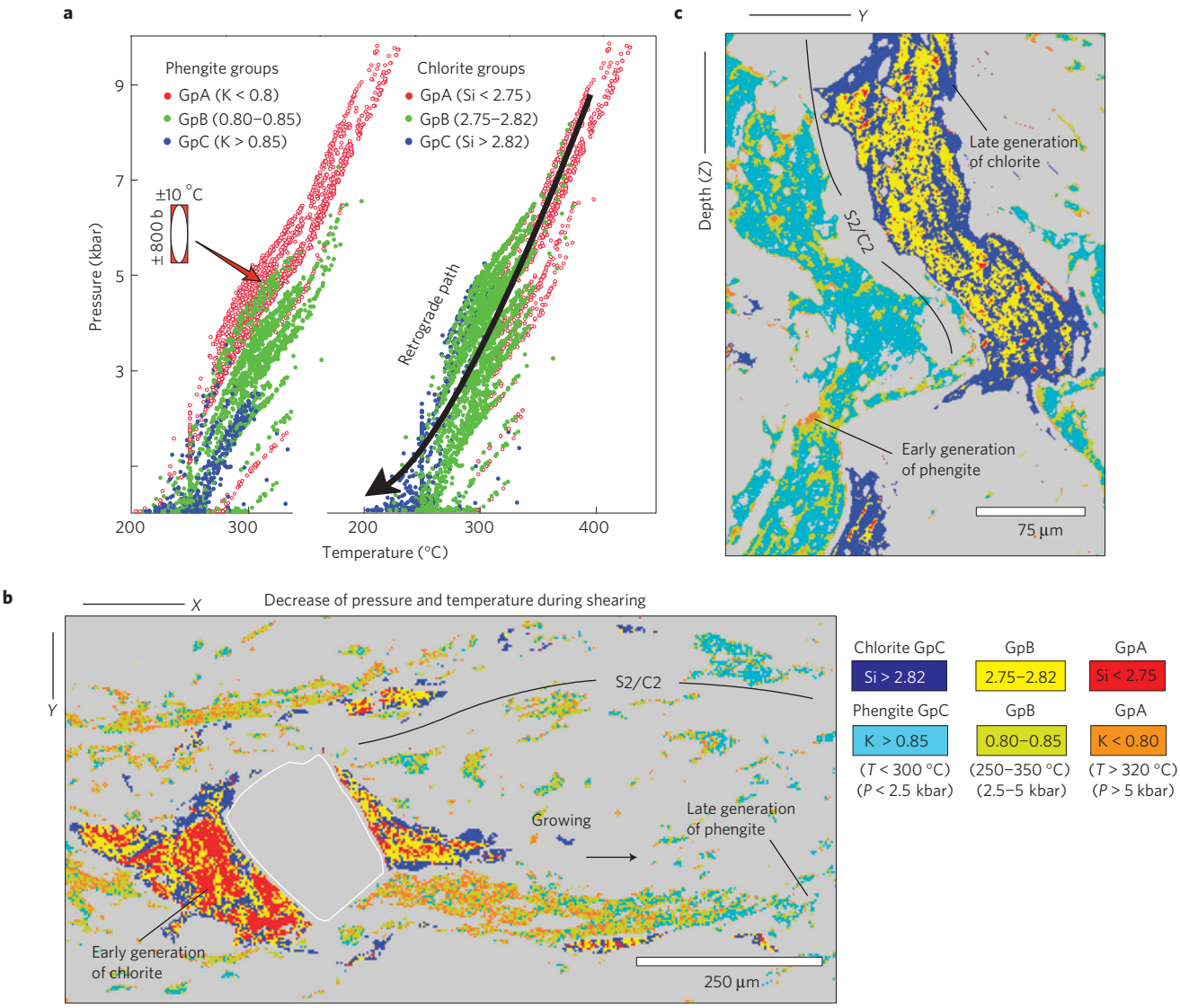

Figure 3 | Chemical evolution of chlorites and phengites during metamorphism in sample Fa-33. a, Plots of K-content in phengite (left) and Si-content in chlorite (right) versus *P*–*T* conditions of equilibria. The *P*–*T* path was calculated from conventional spot analysis. Three groups of chlorite and phengite have been distinguished on the path (GpA, GpB and GpC). **b**,**c**, *P*–*T* maps derived from compositional images obtained in the (*XY*) and (*YZ*) deformation planes. Each chlorite and phengite group is characterized by a specific range of composition, pressure and temperature determined in **a**. The Si-poor chlorites and K-depleted phengites corresponding to the high-*P* group A are mostly observed in the early-formed microstructures.

by GpA, spanning the 5–10 kbar range of pressures. GpA is observed within the S2/C2 shear fabric of the rock, strongly recrystallized and/or mixed with the younger GpB or GpC chlorite/phengite assemblages. This remnant assemblage can also be observed in the pressure shadows of haematite crystals (Fig. 3c). GpA is likely to occur at the early stages of the D2 shear deformation, and possibly during a previous deformation event. Microprobe analyses carried out throughout the rock (3,500 points) argue for a link between the most Si-depleted chlorite (amesite endmember) of GpA and the development of an early fabric termed S1. This early fabric is locally preserved as inclusion trails of chlorite and quartz in the cores of large ankerites (Supplementary Fig. S2). We conclude that the GpA chlorite/phengite assemblage characterizes a transitional domain between two tectono-metamorphic events, termed D1/M1 and D2/M2 in this paper (Fig. 4).

The *P*–*T* stability field of GpA points to a burial of rocks to a minimum depth of 33 km, along a cold geothermal gradient lower than 12 °C km^{-1} (M1). Burial of rocks is likely to have occurred during an early stage of the Eburnean orogeny (D1 event). It was followed by decompression of units associated with a progressive increase of the (M2) gradient from 15 to >50 °C km^{-1} during D2 deformation stages (Fig. 4). To further test the reproducibility of our results, we investigated the D2/M2 event in the high-*T* (up to 450 °C) thermal aureoles of granitoids (Supplementary Fig. S9), from within garnet-bearing micashists. Fourteen samples were studied, among which K451 (Saraya, Sénégal), A11 (Aribinda, Burkina Faso) and Te6C (Tera, Niger) yielded microstructural and petrological evidence that (M2) amphibolite parageneses (garnet–staurolite–chloritoid–cordierite–plagioclase–kyanite–sillimanite–biotite–ilmenite–rutile–quartz) post-dated an early greenschist mineral assemblage (M1) now preserved as inclusion trails of quartz and chlorite in garnet cores. Mineral compositions modelled in Perple-X 0.7 pseudosections[21] were matched with those given by microprobe analysis (Supplementary Figs S10–S16). These results indicate that prograde *P*–*T* paths evolved at rather constant but elevated pressures (6–8 kbar) with increasing temperature (Fig. 4a). It is expected that greenstones were initially deeply buried (~20–25 km) along a cold M1 geothermal gradient,

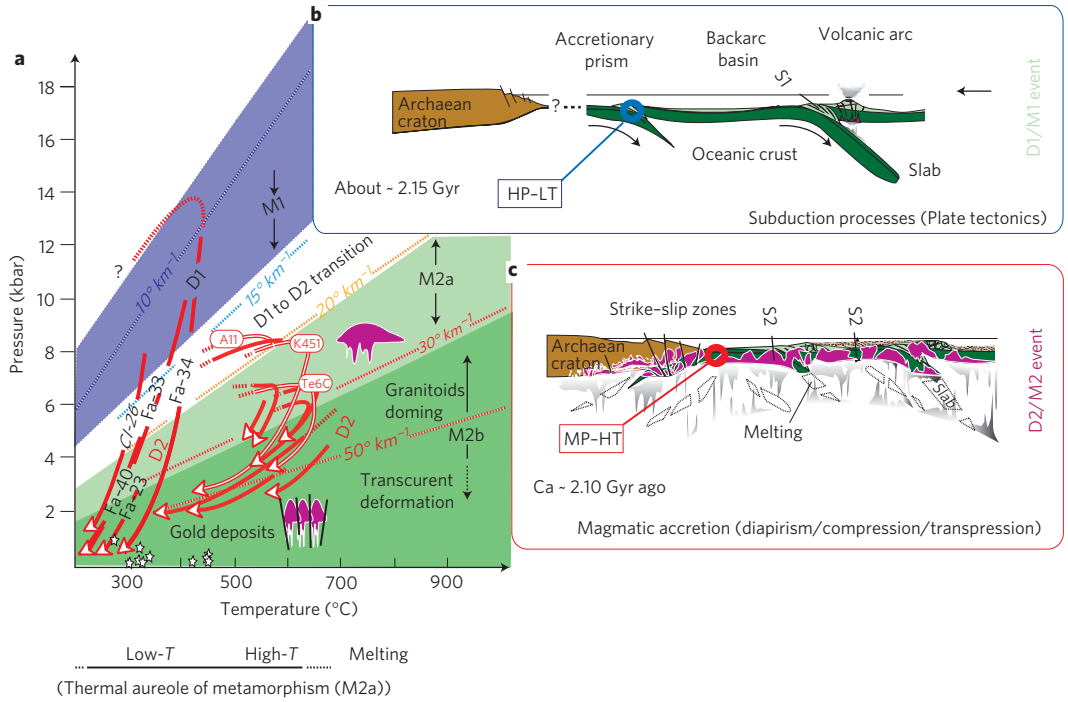

Figure 4 | Inferred geodynamic model endmembers for the Palaeoproterozoic tectonic evolution (2.2–2.0 Gyr ago) of greenstone belts in the WAC. **a**, Metamorphic evolution. **b**, Subduction processes. **c**, Magmatic accretion. Similar *P*–*T* paths (D2/M2) have been derived from high-*T* thermal aureoles of granitoids in the WAC. Nevertheless, a large portion of the *P*–*T* paths from a low-*T* granitoid–greenstone contact (10–12 °C km^{-1}) evolved outside *P*–*T* conditions described by previous authors[28] (from ~15 to 75 °C km^{-1}), but which is similar to paths of supracrustal rocks entering an accretionary prism and subsequently extruded by buoyancy flow during subduction processes (**b**). HP-LT: high-*P*, low-*T*; MP-HT: middle-*P*, high-*T*.

before heating up to ~600–650 °C (close to the solidus of these rocks) during D2-related granitoid emplacement.

Results obtained with two different thermodynamic approaches (multi-equilibrium and pseudosection calculations) using updated and independent thermodynamic databases ('Tweeq' and 'Perple-X', Supplementary Table S2) are consistent and complementary. The issue of matrix fractionation has been addressed in Supplementary Fig. S17. The results yield a coherent metamorphic evolution (from M1 to M2), which reflects a temporal change in the thermal structure of the crust during tectonic activity in the Birimian province.

The main part of this evolution is likely to be related to a long-lived exhumation process (D2 event) of greenstones by emplacement and doming of several generations of granitoids within the newly formed Birimian crust, from 2.15 to 2.0 Gyr ago. Future geochronological studies better constraining the age of metamorphism are needed to further constrain our interpretation. On the basis of the results above, we propose the first interpretation of the metamorphic events recognized along different granitoid–greenstone contacts across the Birimian province. We have investigated several hundred sites (outcrops) and recognized an initial metamorphic phase M1, partially preserved in the low-*T* thermal aureoles of granitoid intrusions and strongly overprinted by M2a/M2b assemblages in the high-*T* ones (Fig. 4a). The difference between M1 and M2 events mainly concerns their calculated peak metamorphic *P* and *T*.

M1 is a relic metamorphic event. It is characterized by an early paragenesis with *T* between 300–450 °C and a low geothermal gradient (10–12 °C km^{-1}) throughout. High-*P* (10–12 kbar), low-*T* (400–450 °C) (HP-LT) chlorite–phengite assemblages have been clearly identified along low-*T* granitoid–greenstone contacts in the Fada N'Gourma area (Fa-33, Fa-34). Similar HP-LT conditions are also expected in the core of greenstone belts (Fa-23, CI-26, Fig. 1). M1 assemblages are linked to a remnant fabric termed S1, probably developed during a short-lived event (D1) and predating, in the eastern Birimian regions (Niger), the about 2.15-Gyr-old major pulse of granitoid intrusions[15].

M2a is a contact metamorphism with a dominant paragenesis indicative of *T* ranging between 250–650 °C and moderate geothermal gradients (20°–30° km^{-1}). M2a assemblages are linked to the regional north-northeast–south-southwest- to northeast–southwest-trending steeply dipping planar S2 fabric and associated with magma intrusion. S2 is likely to result from a long-lived D2 shortening event, probably starting after 2.15 Gyr ago, which shaped the greenstone basins into narrow belts[15]. Middle-*P* (6–8 kbar), high-*T* (550–650 °C) assemblages have been extensively recognized along high-*T* granitoid–greenstone contacts. M2a paths evolved through maximum prograde pressure increases of 1 kbar (see, for example, sample Te6C in Fig. 4a). The retrograde paths, from 8 to <4.0 kbar, define moderately high geothermal gradients of 30–50 °C km^{-1}. It is associated with regional static (cordierite corona around kyanite, Te6C) or dynamic (sigmoid inclusions in staurolite, K451) parageneses, across a large *P*–*T* range and with open clockwise *P*–*T* loops (Fig. 4a).

M2b is also part of the contact metamorphism event but refers to retrogression apparently following on continuously from M2a. It is characterized by abundant chlorite ± phengite crystallization and multiple hydrothermal alteration events linked to mineralized fluids, during a period of exhumation from 2 kbar to <1 kbar with *T* between 200 and 450 °C, and involved elevated geothermal gradients (30–50 °C km^{-1}). M2b assemblages are linked to more localized deformation characterized by a steeply dipping shear fabric named S2/C2 (with both dextral and sinistral shear senses).

The peak *P*–*T* estimate (10–12 kbar, 400–450 °C), related to the early D1/M1 event, corresponds to a blueschist facies series metamorphism, formed along an apparent geothermal gradient of 10–12 °C km^{-1}. This is the oldest documented HP-LT (*T* < 450 °C) metamorphism in the Archaean and Proterozoic record[2].

Previous low apparent geothermal gradients recorded in the Mesoarchaean Barberton greenstone belt (3.2 Gyr old; ref. 24), in the Neoarchaean Belomorian province (2.87 Gyr old; ref. 25) or in the Palaeoproterozoic Tanzania belt (2.0 Gyr old; ref. 26) are all greater than 12–15 °C km^{-1} and correspond to eclogitic mafic rocks formed at T up to 600–700 °C.

It has been suggested that modern-style plate tectonics as characterized by HP-LT (blueschist) and ultrahigh-P metamorphism was globally dominant at the start of the Neoproterozoic[2,27–29]. Our data indicate that HP-LT rocks ($P > 10$ kbar, $T < 450$ °C) already existed in the Palaeoproterozoic and may be preserved in these terrains. This study proposes that the apparent scarcity of old blueschist facies series metamorphism in other parts of the Earth is most likely due to a methodological problem in deciphering P–T evolution within greenstone belts rather than a result of poor preservation[26] or non-existence[2].

Methods

The basic idea of the multi-equilibrium approach is that the ability to resolve pressures and temperatures at thermodynamic equilibrium is improved by increasing the number of endmembers used to express the compositional variability of the phases involved in a given paragenesis. If equilibrium is achieved, all of the independent reactions that can be written in a chemical system must intersect at a single point in the P–T space, corresponding to the P–T conditions of crystallization. It is therefore possible to determine an equilibrium P–T point for high-variance parageneses such as the ones observed in rocks in greenschist belts. This allows a considerably more detailed view of a P–T path evolution.

Numerous studies indicate that the method has the potential to constrain a continuous P–T evolution for meta-pelitic rocks metamorphosed at $T < 550$ °C using a limited number of rock samples[9,10]. For such T conditions, it seems that thermodynamic equilibrium is maintained by crystallizing new chlorite–phengite grains with a composition different from pre-existing minerals, rather than by changing the composition of early grains by lattice diffusion[12,13]. This results in the formation of a mosaic of different local equilibria involving phyllosilicates of various compositions coexisting metastably in a different part of the same thin section. Therefore, different P–T conditions can be calculated from the same sample. Recent studies of meta-pelites, coupling two-dimensional elemental chemical mapping with the multi-equilibria technique, highlight that the spatial distribution at the microscopic scale of these thermodynamic equilibria is governed by deformation[8–10]. The phyllosilicates' composition is correlated with deformation structures such as shear bands, foliation or late cracks. Deformation also steadily disorders the spatial distribution of grains in thermodynamic equilibrium. It follows that minerals that crystallize in contact at a given time are not necessarily in contact by the time the rock reaches the surface. This is illustrated by the P–T-deformation map shown in Fig. 3c, where late chlorite grains crystallized in between cores of earlier chlorites. Phengites are also stretched by deformation. Few former phengite grains are preserved, except in the pressure shadow of the oxide. They appear here partly destabilized and mixed with a later generation. As the determination of chlorite–phengite grains in thermodynamic equilibrium could not be done using simple criteria based on spatial position, equilibrium was checked systematically for all possible Chl–Phg combinations. The P–T conditions calculated for all of the Chl–Phg pairs identified as being in equilibrium with the multi-equilibria technique were plotted in a P–T grid, which leads to the construction of the P–T path of studied samples.

Multi-equilibria calculations were carried out with Matlab using the latest thermodynamic model for phengite[14], which takes into account the T-dependent interlayer water content of dioctahedral mica. About 100,000 Chl–Phg pairs could be treated per day. P–T estimates for the chlorite, phengite, quartz and water parageneses were calculated using the thermodynamic data of five chlorite and six phengite endmembers. These endmembers are Fe-amesite, Mg-amesite, clinochlore, daphnite and sudoite for chlorite, and muscovite, pyrophyllite, hydrated pyrophyllite, Fe-celadonite, Mg-celadonite and phlogopite for phengite. With these endmembers, 359 equilibria can be written for the Chl–Phg–Qtz–water assemblage. Among them, seven are independent. The P–T of equilibrium between Chl, Phg and Qtz, as well as the Fe^{3+} content in chlorite and phengite and the water content of phengite were calculated to minimize the sum of the Gibbs free energy $\sum \Delta G^2$ of seven independent reactions (Supplementary Fig. S5).

In theory, thermodynamic equilibrium is achieved for a given couple if $\sqrt{(\sum \Delta G^2/n_r)}$, where n_r is the number of equilibrium reactions considered, is equal to 0. In practice, a deviation from 0 occurred because of analytical uncertainties. After Monte Carlo simulations[9] (Supplementary Information) accounting for the analytical uncertainties, equilibrium is considered to be achieved when $\sqrt{(\sum \Delta G^2/n_r)} < 2,400$ J for the conventional point analyses, and 4,000 J for the mapping analyses. P–T uncertainties ($\pm 2\sigma$) are estimated to be ± 2.5 kbar/± 15 °C for the mapping mode, and ± 0.8 kbar/± 10 °C for point analyses. These are minimum errors, because these precisions also depend on uncertainties in the thermodynamic state properties of the endmembers and solution models that are hard to estimate.

Calculations involved both point and elemental mapping analyses (475×475 Phg/Chl point analyses for sample Fa-33; 200×200 Phg/Chl mapping analyses for samples Fa-34). Analyses were first filtered on the basis of the compositional criteria[30]. The Fe^{3+} content of phyllosilicates, estimated during the minimization process, has been checked by microscopic X-ray absorption near-edge structure spectroscopy (μ-XANES) measurements carried out at the European Synchrotron Radiation Facility on the ID21 beamline. The thermodynamic estimates and μ-XANES measurement of Fe^{3+} contents in both chlorite and phengite were found to give concordant results. The estimated Fe^{3+}/Fe_{total} ratio ranged from 0.2 to 0.5 for the different generations of chlorite, and from 0.8 to 0.9 for phengite, whereas the values measured on a couple of grains by μ-XANES ranged from 0.16 to 0.45 for chlorites, and was equal to 0.8 for phengites.

Received 23 November 2010; accepted 14 October 2011; published online 20 November 2011

References

1. Maruyama, S., Liou, J. G. & Terabayashi, M. Blueschists and eclogites of the world and their exhumation. *Int. Geol. Rev.* **38,** 485–594 (1996).
2. Stern, R. J. Evidence from ophiolites, blueschists, and ultrahigh-pressure metamorphic terranes that the modern episode of subduction tectonics began in Neoproterozoic time. *Geology* **33,** 557–560 (2005).
3. Cawood, P. A., Kröner, A. & Pisarevsky, S. Precambrian plate tectonics: Criteria and evidence. *GSA Today* **16,** 4–11 (2006).
4. De Wit, M. J. On Archean granites, greenstones, cratons and tectonics: Does the evidence demand a verdict? *Precambr. Res.* **91,** 181–226 (1998).
5. Hamilton, W. B. Archean magmatism and deformation were not products of plate tectonics. *Precambr. Res.* **91,** 143–179 (1998).
6. Davies, G. F. On the emergence of plate tectonics. *Geology* **20,** 963–966 (1992).
7. Bjørnerud, M. G. & Austrheim, H. Inhibited eclogite formation: The key to the rapid growth of strong and buoyant Archean continental crust. *Geology* **32,** 765–768 (2004).
8. De Andrade, V., Vidal, O., Lewin, E., O'Brien, P. & Agard, P. Quantification of electron microprobe compositional maps of rock thin sections: An optimized method and examples. *J. Metamorph. Geol.* **24,** 655–668 (2006).
9. Vidal, O. *et al.* P–T-deformation-Fe^{3+}/Fe^{2+} mapping at the thin section scale and comparison with XANES mapping. Application to a garnet-bearing metapelite from the Sambagawa metamorphic belt (Japan). *J. Metamorph. Geol.* **24,** 669–683 (2006).
10. Yamato, P. *et al.* New, high-precision P–T estimates for Oman blueschists: Implications for obduction, nappe stacking and exhumation processes. *J. Metamorph. Geol.* **25,** 657–682 (2007).
11. Perchuk, L. L. *et al.* Comparative petrology and metamorphic evolution of the Limpopo (South Africa) and Lapland (Fennoscandia) high-grade terrains. *Mineral. Petrol.* **69,** 69–107 (2000).
12. Vidal, O., Parra, T. & Trotet, F. A thermodynamic model for Fe–Mg aluminous chlorite using data from phase equilibrium experiments and natural pelitic assemblages in the 100–600 °C, 1-25 kbar P–T range. *Am. J. Sci.* **301,** 557–592 (2001).
13. Parra, T., Vidal, O. & Agard, P. A Thermodynamic model for Fe–Mg dioctahedral K-white micas using data from phase equilibrium experiments and natural pelitic assemblages. *Contrib. Mineral. Petrol.* **143,** 706–732 (2002).
14. Dubacq, B., Vidal, O. & De Andrade, V. Dehydration of dioctahedral aluminous phyllosilicates: Thermodynamic modelling and implications for thermobarometric estimates. *Contrib. Mineral. Petrol.* **159,** 159–174 (2010).
15. Baratoux, L. *et al.* Juvenile Paleoproterozoic crust evolution during the Eburnean orogeny (~2.2–2.0 Gyr), western Burkina Faso. *Precambr. Res.* **191,** 18–45 (2011).
16. Doumbia, S. *et al.* Petrogenesis of juvenile-type Birimian (Paleoproterozoic) granitoids in Central Côte-d'Ivoire, west Africa: Geochemistry and geochronology. *Precambr. Res.* **87,** 33–63 (1998).
17. Dioh, E., Béziat, D., Debat, P., Grégoire, M. & Ngom, M. Diversity of the Paleoproterozoic granitoids of the Kédougou inlier (eastern Sénégal): Petrographical and geochemical constraints. *J. Afr. Earth Sci.* **44,** 351–371 (2006).
18. Bonhomme, M. Contribution à l'étude géochronologique de la plate-forme de l'Ouest Africain. *Ann. Fac. Sci. Univ. Clermont-Ferrand* **5** (1962).
19. Feybesse, J-L. *et al.* The paleoproterozoic Ghanaian province: Geodynamic model and ore controls, including regional stress modelling. *Precambr. Res.* **149,** 149–196 (2006).
20. Vegas, N., Naba, S., Bouchez, J-L. & Jessell, M. Structure and emplacement of granite plutons in the Paleoproterozoic crust of Eastern Burkina Faso: Rheological implications. *Int. J. Earth Sci.* **97,** 1165–1180 (2007).
21. Berman, R. G. Thermobarometry using multi-equilibrium calculations: A new technique, with petrological applications. *Can. Mineral.* **29,** 833–855 (1991).

22. Powell, R. & Holland, T. J. B. Optimal geothermometry and geobarometry. *Am. Mineral.* **79,** 120–133 (1994).
23. Connolly, J. A. D. The geodynamic equation of state: What and how. *Geochem. Geophys. Geosyst.* **10,** q10014 (2009).
24. Moyen, J-F., Stevens, G. & Kisters, A. Record of mid-Archaean subduction from metamorphism in the Barberton terrain, South Africa. *Nature* **442,** 559–562 (2006).
25. Mints, M. V. *et al*. Mesoarchean subduction processes: 2.87 Ga eclogites from the Kola Peninsula, Russia. *Geology* **38,** 739–742 (2010).
26. Möller, A., Appel, P., Mezger, K. & Schenk, V. Evidence for a 2 Ga subduction zone: Eclogites in the Usagaran belt of Tanzania. *Geology* **23,** 1067–1070 (1995).
27. Condie, K. C & Kröner, A. in *When Did Plate Tectonics Begin on Planet Earth?* Vol. 440 (eds Condie, K. C. & Pease, V.) 281–294 (GSA, 2008) (special issue).
28. Brown, M. D. in *When Did Plate Tectonics Begin on Planet Earth?* Vol. 440 (eds Condie, K. C. & Pease, V.) 97–128 (GSA, 2008) (special issue).
29. Ernst, W.G. Archean plate tectonics, rise of Proterozoic supercontinentality and onset of regional, episodic stagnant-lid behaviour. *Gondwana Res.* **15,** 243–253 (2009).
30. Vidal, O. & Parra, T. Exhumation paths of high pressure metapelites obtained from local equilibria for chlorite–phengite assemblages. *Geol. J.* **35,** 139–161 (2000).

Acknowledgements

The project was financially supported by IRD and INSU-CNRS. We thank the ID21 beamline staff at the ESRF for providing us with beam time that supported our calculations by *in situ* measurements. We also acknowledge the team of the AMIRA P934 project for logistic support in Burkina Faso. B. Goscombe, D. Chardon and J.-L. Bouchez are thanked for comments and discussions.

Author contributions

J.G. conceived the study and wrote the paper. V.D.A. and J.G. contributed equally to the petrologic analysis and metamorphic modelling. R.F.W. and V.D.A. helped generate the research idea with J.G. and contributed to the writing and focusing of the paper. B.D. and O.V. provided the most updated solid-solution models for chlorite and phengite. All authors contributed to the interpretation of these results within the greenstone belts of the WAC.

Additional information

The authors declare no competing financial interests. Supplementary information accompanies this paper on www.nature.com/naturegeoscience. Reprints and permissions information is available online at http://www.nature.com/reprints. Correspondence and requests for materials should be addressed to J.G.